Supplementary Materials for

Reduced vaccination and the risk of measles and other childhood infections post-Ebola

Saki Takahashi, C. Jessica E. Metcalf, Matthew J. Ferrari, William J. Moss, Shaun A. Truelove, Andrew J. Tatem, Bryan T. Grenfell and Justin Lessler

Correspondence to: justin@jhu.edu

This PDF file includes:

1. Materials and Methods

1.1 Vaccination Maps

Measles vaccination status from individuals 0 to 59 months of age in 1,054 geo-located geographic clusters was obtained from Demographic and Health Surveys (DHS) conducted in 2013 (Liberia, Sierra Leone) and 2012 (Guinea) and made publicly available by ICF International (*22*). DHS survey locations are shown in Figure S1. Recent DHS surveys from countries surrounding the Ebola affected countries were also obtained: Senegal (2010-2011), Mali (2012-2013), and Cote d'Ivoire (2011-2012). Each individual was reported as having an exact time of the first dose of measles-containing vaccine (MCV-1) vaccination (vaccination card), known previous MCV-1 vaccination (mother's report), or having not received MCV-1 vaccination. Data on the timing and geographic target of supplemental immunization activities (SIAs) was made available by the WHO.

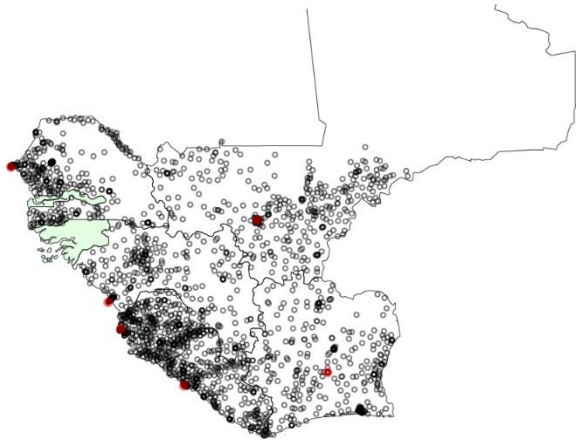

Fig. S1. DHS survey locations (grey circles) in Guinea, Liberia, Sierra Leone, and neighboring countries. Capital cities are shown in red.

The likelihood of each individual over 8.5 months of age's observed vaccination status was modelled based on a location specific saturating survival (and corresponding probability density) function:

$$L(\boldsymbol{\theta_j}; y_{ij}) = f(t_{ij}; \boldsymbol{\theta_j})^{\epsilon_{ij}} \, S(t_{ij}; \boldsymbol{\theta_j})^{r_{ij}} \, \left(1 - S(t_{ij}; \boldsymbol{\theta_j})\right)^{\ell_{ij}} \quad \textbf{(1)}$$

where t_{ij} is the known exact age of vaccination or age of censoring for individual i at location j, $S(t_{ij}; \boldsymbol{\theta_j})$ is the survival function for parameters $\boldsymbol{\theta_j}$ at location j, $f(t_{ij}; \boldsymbol{\theta_j})$ is the corresponding probability density function (pdf), and ϵ_{ij}, ℓ_{ij}, and r_{ij} are indicators of whether the observation was observed exactly, left censored, or right censored, respectively. The survival function and pdf are characterized as:

$$S(t_{ij}; \boldsymbol{\theta_j}) = 1 - \left[p_j(1 - e^{-\lambda_j(t_{ij} - 8.5)})\right]\left[1 - \prod_{k=1}^{m} \rho_{kj}^{c_{ijk}}\right] \quad \textbf{(2)}$$

$$f(t_{ij}; \boldsymbol{\theta_j}) = p_j \lambda_j \, e^{-\lambda_j(t_{ij} - 8.5)} \quad \textbf{(3)}$$

where p_j is the probability of ever being vaccinated through the routine program over the course of your life if you live at location j (e.g., the saturation parameter), λ_j is the rate at which individuals at that location who eventually receive routine vaccination are vaccinated (after coming into risk at 8.5 months of age), ρ_{kj} is the probability of being vaccinated in SIA campaign k at location j, and c_{ijk} is an indicator of individual i in location j's eligibility for campaign k.

All parameters are fit in an MCMC framework (the Stan modelling language (*26*)) using non-informative priors and are considered to be random effects from a spatial process of the form:

$$\theta_{jx} \sim N\left(\sum_{l \neq j}\left(\theta_{lx} \times {d_{j,l}}^{-2}\right) / \sum_{l \neq j}\left({d_{j,l}}^{-2}\right), \sigma^2\right) \quad \textbf{(4)}$$

where $d_{j,l}$ is the distance between j and l. Each of the spatial vaccination parameters is assumed to come from an independent spatial process such that $\lambda_j = \exp(\theta_{j1}), p_j = logistic(\theta_{j2})$, and $\rho_{jk} = logistic(\theta_{j3k})$.

Expected vaccination rates (e.g., parameters) were then determined for the entire country by laying a 5 km x 5 km grid across the country and interpolating the expected value for each grid cell given its relationship to the centroids by application of equation **(4)** above. Spatially explicit vaccination rates, converted to the probability of receiving routine vaccination by 2 years of age, are shown in Figure S2.

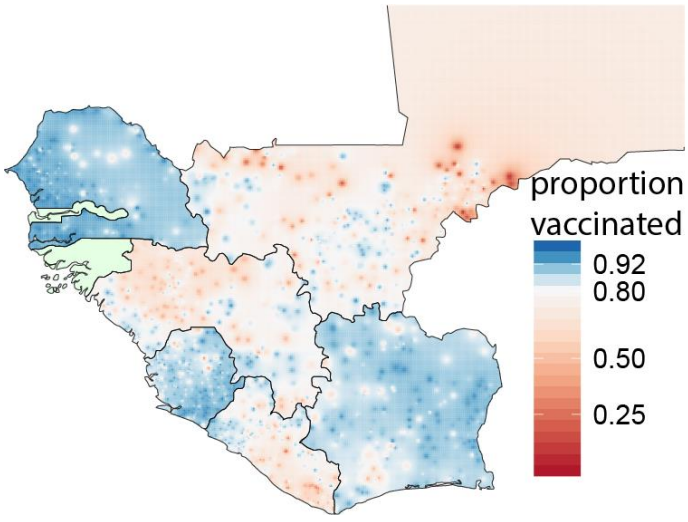

Fig. S2. Probability of receiving routine measles vaccination by 2 years of age in the absence of health care disruptions.

Data on birth rates and the population distributions by age were obtained from the WorldPop project (www.worldpop.org.uk). High resolution satellite data on mapped human settlements were combined with land use information to disaggregate detailed annual numbers of live births and census counts by 5 year age groups to a spatial resolution of approximately 100 m x 100 m. These WorldPop datasets were used to determine the expected number of unvaccinated children 9 to 59 months of age in each

grid cell. Projections for the number unvaccinated after 6, 12, and 18 months of disruptions were calculated by reducing the routine vaccination rate λ_j by 75% (e.g., the primary scenario), and then projecting forward based on the birth rate.

National vaccination rates and saturation parameters of the first dose of diphtheria-tetanus-pertussis (DTP-1) as a proxy for pentavalent vaccine, Bacillus-Calmette-Guérin (BCG), and oral polio vaccine (OPV) were estimated using the likelihood framework as in equation **(1)** above and disruptions were simulated similarly as for measles.

1.2 Lexis Diagrams and Full Population Immunity

The age distribution of measles susceptibility at the national scale for each of the Ebola affected countries was obtained using a simple model where each age cohort's immunity is estimated based on its experience of routine immunization, SIAs, and natural infection. For example, if 80% of the cohort was routinely vaccinated and the cumulative measles attack rate was 75% among those unvaccinated, 95% of the cohort would be estimated to be immune.

Routine and SIA coverage rates were assumed to be the WHO reported administrative estimates (*6*); we also assumed complete overlap between the probability of routine and SIA vaccination (so that where a cohort had experienced vaccination via an SIA as well as routine vaccination, coverage in that cohort was taken to be the highest of the two values), and a maximum coverage of 95% in both SIAs and routine immunization. For those born between 2012 and 2015, we used estimates from the spatial models described above (fit to DHS data) with and without Ebola related vaccine disruptions. Although vaccination coverage reported to the WHO is often overestimated (*27*), most unvaccinated individuals in older age groups (where DHS estimates are not available) are likely to have experienced natural immunity which is also accounted for (see below), so this should have minimal impacts on our final results.

The probability of natural immunity as a function of age was estimated by assuming a constant hazard of infection in all age classes; the base hazard rate in 1980 was set such that 95% of infections occur prior to 20 years of age;

$$P(\text{infection by age } a) = 1 - exp(-0.149 \times a) \quad \textbf{(5)}$$

and the base hazard rate in subsequent years was then scaled relative to the proportional decline in estimated measles incidence in each year relative to 1980; e.g., the hazard rate in year t = 0.149 × (incidence in year t / incidence in 1980). Estimated measles incidence was taken from the 2013 WHO measles burden estimates, calculated as per Simons *et al*. (*5*).

Resulting profiles reflect relatively low levels of susceptibility in the population (e.g., 5.4% across the 3 countries, see supplement section 1.3), in line with expectations from the combined impact of vaccination with natural immunity, which in pre-vaccination populations can result in susceptibility profiles of around 3% (*28*).

1.3 Estimating Measles Attack Rates

Estimating the transmission rate of measles at the country scale is complicated by the high degree of spatial heterogeneity in population density, access to health care, and movement. Applying local scale estimates of the effective reproductive ratio, R_e, to the country scale using standard, mean-field SIR type models tends to grossly over-estimate the potential size of outbreaks because of the implicit assumption that all individuals are equally exposed to infection.

Simons *et al.* used an extended Kalman filter model to estimate an annualized measles attack rate as a function of the proportion susceptible to measles in the population from national level, annual reported measles cases. The Kalman filter model fits a semi-parametric, dynamic transmission model to the unobserved, true measles incidence, filtered through an observation model that simultaneously estimates the under-reporting in the observed cases (for more details see (*5*) and (*29*)). Simons *et al.* presented estimates using annual measles cases from 1980 to 2009; here, we have updated those estimates using reported measles cases from 1980 to 2012. The functional form of the attack rate A, defined as the proportion of susceptibles that become infected per year, is given as:

$$A = 1 - exp\left(-\theta \times \frac{S}{N}\right) \quad \textbf{(6)}$$

where S is the number of individuals susceptible to measles in the population and N is the population size. We estimated the quantity θ independently for each country in the WHO African region using observations of reported measles cases from 1980 to 2011. To estimate the attack rate in the Ebola affected region, we took the mean of the distribution of parameter estimates for the African region (θ_{mean} = 4.72), and low and high scenarios corresponding to the 25th (θ_{low} = 2.53) and 75th (θ_{high} = 5.77) percentiles of the distribution of estimates for the African region.

Our projection of the number of susceptibles following 18 months of disruptions in vaccination due to the Ebola outbreak suggests that 5.4% of the total population is likely to be susceptible to measles. This corresponds to a predicted attack rate of 18.8% of susceptibles per year, with low and high predictions of 12.7% and 26.6%, respectively (Figure S3).

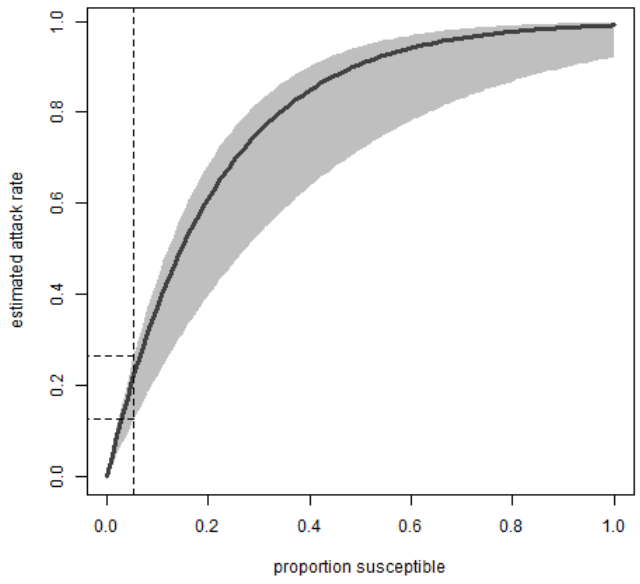

Fig. S3. Predicted mean annual measles attack rate as a function of the proportion susceptible (e.g., not immune to measles) in the population (solid line). Grey shading gives the range of predictions for the low and high scenarios (corresponding to the 25th and 75th percentiles of the distribution of transmission rates for the African region). The vertical dashed line indicates the estimated 5.4% of the population susceptible to measles following 18 months of disruptions of vaccination due to the Ebola outbreak; horizontal dashed lines indicate the corresponding upper and lower projections of the annual attack rate.

1.4 Estimating Measles Associated Mortality

Expected measles associated mortality in an outbreak was calculated by taking the number of susceptibles over the entire country estimated using the Lexis diagram, and applying an expected attack rate using the method described above. We then applied the expected case fatality ratio (CFR) for outbreak settings as reported in Wolfson *et al.* to obtain the total number of deaths (*15*). Based on the source population for these estimates, a uniform CFR is assumed across age ranges. Table S1 shows estimates of the total mortality spanning the confidence limits on each estimate. Wolfson *et al.* project an overall CFR of 5-6% for Guinea, Liberia, and Sierra Leone, in accord with the mid-line outbreak level estimate. Plausible ranges are based on the implied number of deaths at the limits of the inter-quartile prediction intervals for measles attack rates, and the low and high end of the range of CFR estimates reported for outbreak settings in Wolfson *et al*.

Table S1. Projected measles mortality under different levels of attack rates and case fatality ratios (CFRs) with and without 18 months of disruptions in normal vaccination activities. Numbers in bold show the limits of the plausible range of deaths shown in the text.

			CFR		
Baseline Attack Rate (3.9% susceptible)		**Projected Cases**	*low*	*median*	*high*
			0.0256	0.0518	0.1155
25th percentile	0.095	84833	**2172**	4394	9798
median	0.142	126868	3248	**6572**	14653
75th percentile	0.204	181679	4651	9411	**20984**
18m Disruption Attack Rate (5.4% susceptible)					
25th percentile	0.127	153458	**3929**	7949	17724
median	0.188	227484	5822	**11781**	26267
75th percentile	0.266	321702	8236	16664	**37157**

1.5 Maternal Mortality

The yearly increase in deaths from an increase in maternal mortality to 2000 levels was calculated using maternal mortality data obtained from the WHO (*30*). Year 2013 and year 2000 maternal mortality ratios (MMRs) were applied to year 2013 rates of live births for each country. The difference between applying the year 2000 and year 2013 MMRs was calculated for each country, and these differences were summed to determine the overall expected increase in mortality.

All analysis was conducted using the R statistical software, version 3.0.2 (*31*).

2. Supplementary Text

2.1 Alternate Scenarios

In order to assess the effects of more geographically focused and less severe disruptions, we considered four additional scenarios: 75% reductions in national vaccination rate confined to the areas most affected by the Ebola outbreak (top 50% of incidence by district), smaller reductions in vaccination rates (25% and 50%), and complete disruption of vaccination (100%). Resulting distributions of vaccination and a map after 18 months of Ebola specific disruptions are shown in Table S2 and Figure S4. Ebola incidence rates were based on situation reports publicly available as of January 16, 2015 from the French Embassy in Conakry (Guinea) (*24*), the Ministry of Health & Social Welfare of Liberia (*25*), and the Ministry of Health and Sanitation of Sierra Leone (*26*).

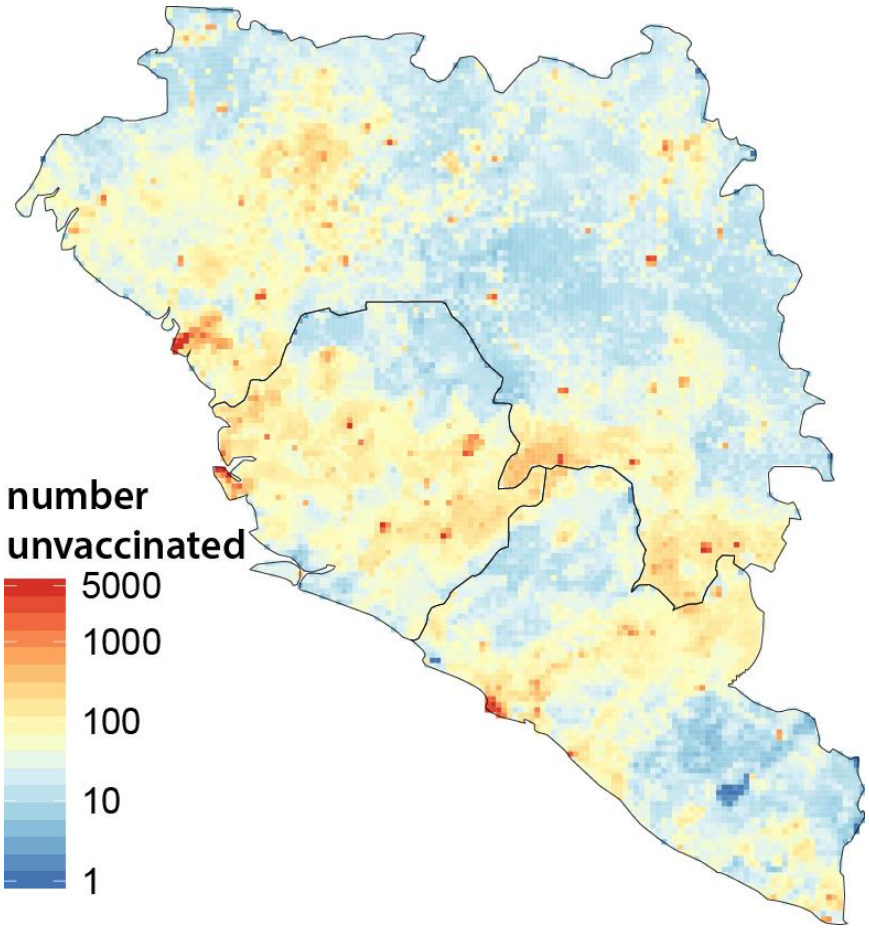

Fig. S4. Number of children 9 to 59 months of age not vaccinated against measles in Guinea, Liberia, and Sierra Leone after 18 months if measles disruptions were confined to the 50% of districts with the highest Ebola incidence rate (per 1,000).

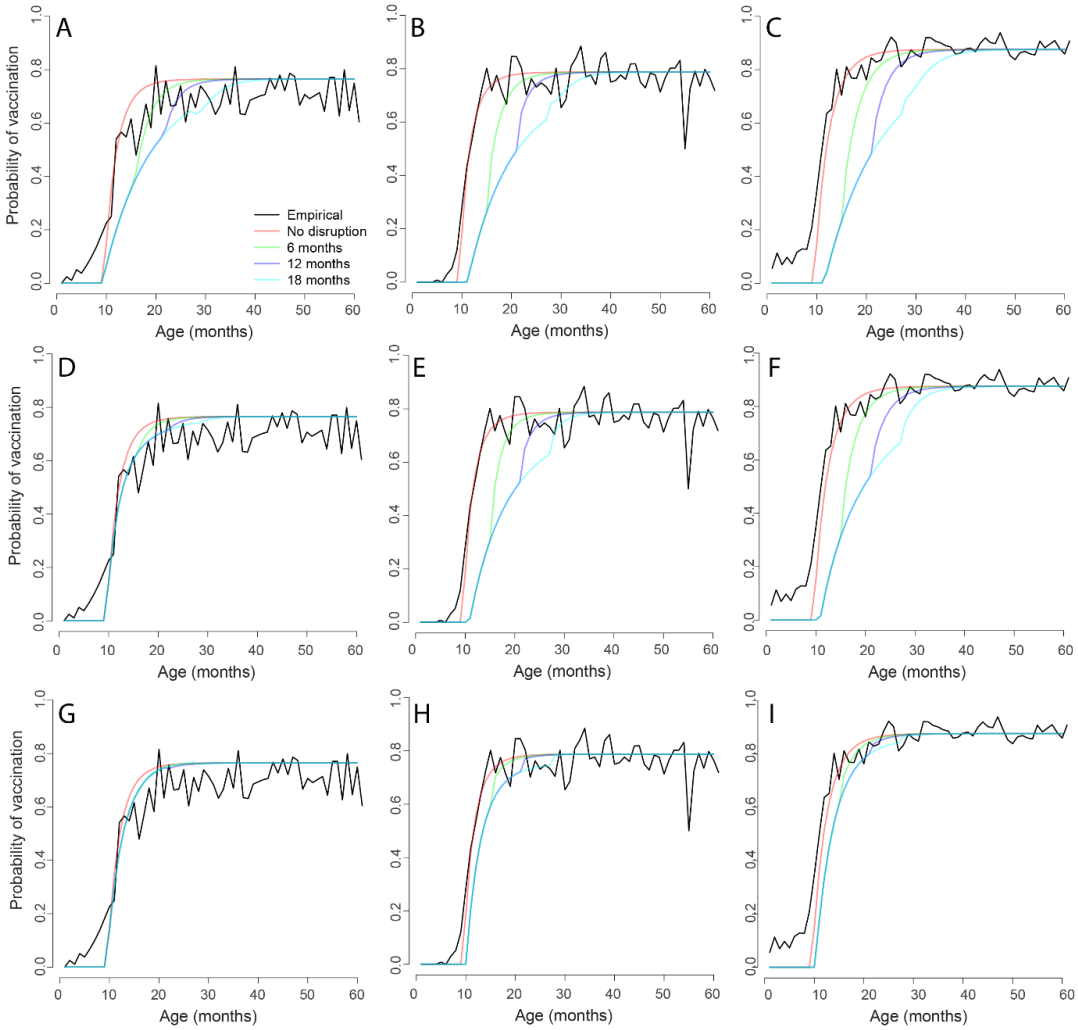

Fig. S5. Comparison of weighted proportion vaccinated by age observed in the DHS data (black line) in **(A)** Guinea, **(B)** Liberia, and **(C)** Sierra Leone with baseline model projections and primary disruption scenario; **(D)** Guinea, **(E)** Liberia, and **(F)** Sierra Leone with 18 months of disruptions confined to 50% of districts with the highest Ebola incidence rate (per 1,000); and **(G)** Guinea, **(H)** Liberia, and **(I)** Sierra Leone with 25% reductions in vaccination rate. Curves show the trajectory of scenarios including no disruption (red), and projections after 6 months (green), 12 months (purple), and 18 months (turquoise) of disruptions.

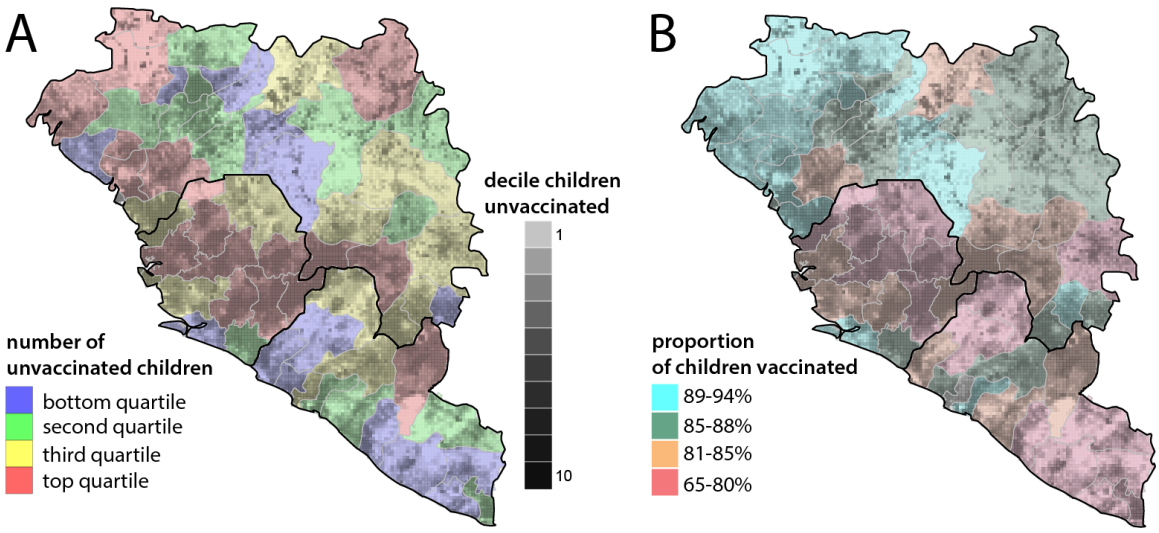

Fig. S6. (A) The number of children 9 to 59 months of age not vaccinated against measles per district (colors by quartile class) and **(B)** the proportion of children 9 to 59 months of age vaccinated against measles per district (colors by quartile class), overlaid on the number of children 9 to 59 months of age not vaccinated against measles in Guinea, Liberia, and Sierra Leone after 18 months of disruptions (grayscale by decile class).

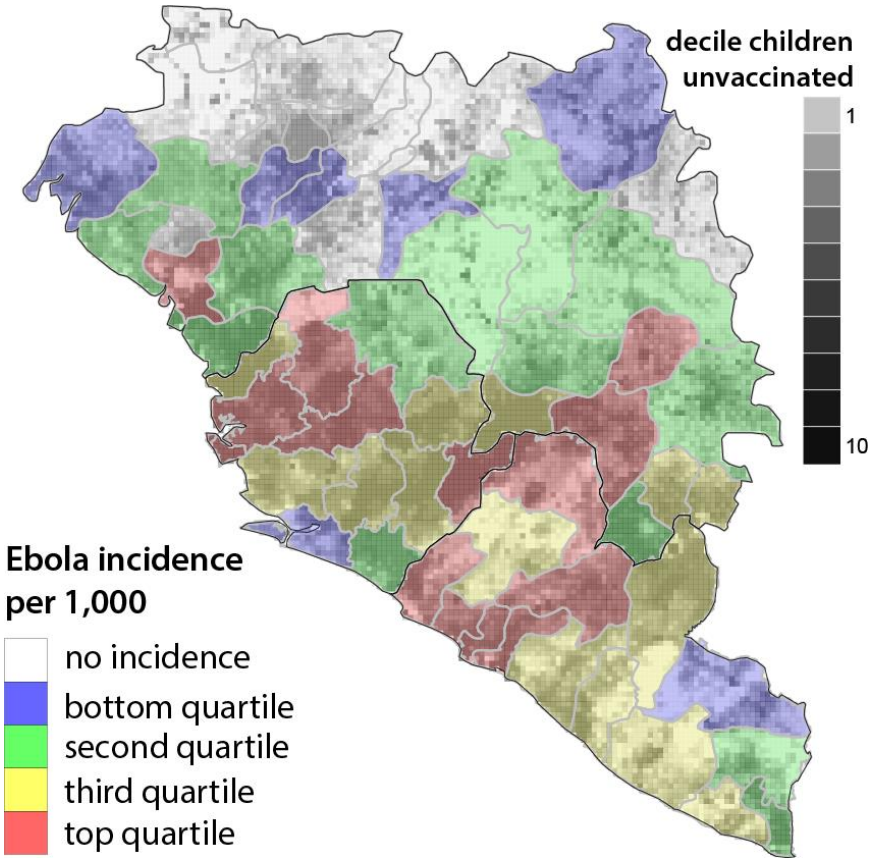

Fig. S7. Ebola incidence rate (per 1,000) (colors by quartile class) overlaid on the number of children 9 to 59 months of age not vaccinated against measles in Guinea, Liberia, and Sierra Leone after 18 months of disruptions (grayscale by decile class).

Table S2. Projected unvaccinated population sizes, measles susceptibility, outbreak sizes, and deaths under alternate vaccination scenarios: primary scenario, 75% reductions in vaccination rates only in the 50% of districts with the highest Ebola incidence rate (per 1,000), and 25%, 50%, and 100% reductions in national vaccination rates.

	Primary scenario	**Disruptions in only most affected Ebola districts**	**25% reductions in vaccination rate**	**50% reductions in vaccination rate**	**100% reductions in vaccination rate**
Unvaccinated children 9-59 months of age					
No disruptions	778,124 (714,897 - 915,159)	778,124 (714,897 - 915,159)	778,124 (714,897 - 915,159)	778,124 (714,897 - 915,159)	778,124 (714,897 - 915,159)
6 months of disruptions	964,346 (862,682 - 1,129,026)	887,500 (803,670 - 1,039,717)	825,926 (746,029 - 980,775)	880,246 (785,695 - 1,045,647)	1,100,580 (1,037,357 - 1,237,356)
12 months of disruptions	1,068,833 (914,108 - 1,288,857)	950,029 (836,879 - 1,132,893)	837,421 (750,291 - 1,010,629)	915,027 (797,378 - 1,120,191)	1,423,032 (1,359,817 - 1,559,338)
18 months of disruptions	1,129,376 (934,926 - 1,409,052)	987,075 (851,417 - 1,203,106)	842,039 (753,034 - 1,025,409)	928,884 (801,606 - 1,164,014)	1,745,472 (1,682,277 - 1,880,846)
24 months of disruptions	1,165,633 (944,883 - 1,499,853)	1,009,886 (858,984 - 1,256,321)	845,150 (755,631 - 1,033,627)	935,696 (804,552 - 1,190,586)	2,067,871 (2,004,737 - 2,201,246)
Population Susceptibility					
No disruptions	891,231	891,231	891,231	891,231	891,231
18 months of disruptions	1,209,210	1,091,810	960,637	1,043,269	1,584,166
Outbreak Size					
No disruptions	126,868 (84,833 - 181,679)	126,868 (84,833 - 181,679)	126,868 (84,833 - 181,679)	126,868 (84,833 - 181,679)	126,868 (84,833 - 181,679)
18 months of disruptions	227,484 (153,458 - 321,702)	187,229 (125,915 – 266,039)	146,542 (98,184 - 209,285)	171,646 (115,276 – 244,354)	378,414 (258,040 – 527,792)
Deaths					
No disruptions	6,572 (2,172 - 20,984)	6,572 (2,172 - 20,984)	6,572 (2,172 - 20,984)	6,572 (2,172 - 20,984)	6,572 (2,172 - 20,984)
18 months of disruptions	11,781 (3,929 - 37,157)	9,698 (3,223 – 30,728)	7,519 (2,514 - 24,172)	8,891 (2,951 – 28,223)	19,602 (6,606 – 60,960)